ORIGINAL ARTICLE

IWJ WILEY

Pyridoxamine ameliorates methylglyoxal-induced macrophage dysfunction to facilitate tissue repair in diabetic wounds

Minfei Jiang | **Aobuliaximu Yakupu** | **Haonan Guan** | **Jiaoyun Dong** | **Yingkai Liu** | **Fei Song** | **Jiajun Tang** | **Ming Tian** | **Yiwen Niu** | **Shuliang Lu**

Department of Burn, Ruijin Hospital, Shanghai Jiao Tong University School of Medicine, Shanghai, China

Correspondence
Ming Tian, MD, Yiwen Niu, MD, and Shuliang Lu, MD, PhD, Shanghai Burn Institute, Ruijin Hospital, Shanghai Jiao Tong University School of Medicine, No. 197 Ruijin Er Road, Shanghai 200025, China.
Email: tianming198@163.com (M. T.),
Email: 13636489036@163.com (Y. N.),
and
Email: 13901738685@139.com (S. L.)

Abstract

Methylglyoxal (MGO) is a highly reactive dicarbonyl compound formed during hyperglycaemia. MGO combines with proteins to form advanced glycation end products (AGEs), leading to cellular dysfunction and organ damage. In type 2 diabetes mellitus (T2DM), the higher the plasma MGO concentration, the higher the lower extremity amputation rate. Here, we aimed to identify the mechanisms of MGO-induced dysfunction. We observed that the accumulation of MGO-derived AGEs in human diabetic wounds increased, whereas the expression of glyoxalase 1 (GLO1), a key metabolic enzyme of MGO, decreased. We show for the first time that topical application of pyridoxamine (PM), a natural vitamin B6 analogue, reduced the accumulation of MGO-derived AGEs in the wound tissue of type-2 diabetic mice, promoted the influx of macrophages in the early stage of tissue repair, improved the dysfunctional inflammatory response, and accelerated wound healing. In vitro, MGO damaged the phagocytic functions of M1-like macrophages induced by lipopolysaccharide (LPS), but not those of M0-like macrophages induced by PMA or of M2-like macrophages induced by interleukins 4 (IL-4) and 13 (IL-13); the impaired phagocytosis of M1-like macrophages was rescued by PM administration. These findings suggest that the increase in MGO metabolism in vivo might contribute to macrophage dysfunction, thereby affecting wound healing. Our results indicate that PM may be a novel therapeutic approach for treating diabetic wounds. MGO forms protein adducts that cause macrophage dysfunction. These adducts cause cell and organ dysfunction that is common in diabetes. Pyridoxamine scavenges MGO to ameliorate this dysfunction, promoting wound healing. Pyridoxamine could be used therapeutically to treat non-healing diabetic wounds.

1 | INTRODUCTION

According to the 2019 prevalence data from the International Diabetes Federation, lower extremity complications of diabetic foot influence 40 to 60 million diabetic patients worldwide.[1] It has been estimated that, globally, a lower limb is fully or partially lost to amputation every 30 seconds as a consequence of diabetes.[2] However, the precise molecular mechanisms through which type 2 diabetes mellitus (T2DM) results in impaired wound healing remain unknown.

Methylglyoxal (MGO) is a highly reactive dicarbonyl compound formed during hyperglycaemia and is the most important precursor in the spontaneous modification of proteins and nucleic acid molecules, resulting in the generation of advanced glycation end products (AGEs).[3,4] The glycation capacity of MGO is ~20 000 times higher than that of glucose.[5] MGO mainly reacts with the arginine residues of proteins,[6,7] which are usually present in the functional domains; this modification induced by MGO contributes to alterations in cellular proteins and results in cellular dysfunction, subsequently leading to various health problems. A recent clinical study showed that the amputations rate of lower extremity in T2DM patients is connected to an elevation of MGO levels in the plasma,[8] providing evidence of the role of MGO in persistent foot ulcerations. Normally, more than 99% of MGO is detoxicated by glyoxalase,[9,10] through which MGO is converted to D-lactate,[11] with glyoxalase 1 (GLO1) as the rate-limiting enzyme.[12] Prolonged exposure to MGO leads to microvascular damage and impaired wound healing.[13] In diabetic mice, treatment with the small-molecule formulation of GLO1 induced the acceleration of wound healing via trans-resveratrol- and hesperetin-mediated pathways by enhancing angiogenesis.[14] These phenomena indicate that the quenching of MGO could accelerate the healing of diabetic wounds.

Macrophages play a pivotal role in wound repair[15,16]; in the early stage, they secrete inflammatory cytokines and aid in the clearance of pathogens and environmental debris, whereas in the later stage of wound healing, macrophages help to resolve inflammation and promote tissue repair.[17,18] Thus, macrophages play a dual role, as they not only contribute to tissue destruction, but they also promote later repair.[19] Disturbances in macrophage function can lead to aberrant repair mechanisms.[20] In diabetic mice, increased AGE formation results in

impaired macrophage infiltration and phagocytosis,[21] leading to prolonged inflammation and impaired wound healing. We speculate that MGO, as the most important precursor of AGEs, might be a critical factor in regulating macrophage dysfunction in the process of diabetic wound repair.

Pyridoxamine (PM) is the most important scavenger of MGO,[22] which can reduce MGO-induced glycation.[23] In a clinical trial in T2DM patients with overt nephropathy, PM restrained the accumulation of AGEs and ameliorated kidney function.[24] In another clinical trial, PM administration reduced the accumulation of AGEs and inhibited inflammation in osteoarthritis patients.[25] In diabetic mouse models, impaired glucose metabolism was restrained by PM administration.[26] Overall, these discoveries emphasise the latent role of PM as an antiglycating agent that acts via the targeting of MGO. Thus, we aimed to determine the mechanisms through which MGO induces such dysfunction and to determine how PM can protect against these changes.

2 | MATERIALS AND METHODS

2.1 | Human subjects

This research included patients who were diagnosed with T2DM who had non-healing wounds on the lower limbs lasting at least 3 months. The diabetic wound tissue (n = 3) was collected through the debridement or amputation of non-healing lower limb wounds. The wound tissue from healthy patients (n = 3) was obtained during debridement following acute traumatic injury; in such

---

Key Messages

- methylglyoxal (MGO) forms protein adducts that cause macrophage dysfunction
- these adducts cause cell and organ dysfunction that is common in diabetes
- pyridoxamine scavenges MGO to ameliorate this dysfunction, promoting wound healing
- pyridoxamine could be used therapeutically to treat non-healing diabetic wounds

cases, the tissue was removed from the margin of the wound. Residual full-thickness skin grafts were obtained from the abdominal skin of patients with T2DM (n = 3) and non-diabetic (n = 3) patients who were admitted to the hospital to undergo plastic and reconstructive surgeries. Each patient provided informed consent. All procedures involving human subjects were approved by the Ethics Review Board of Ruijin Hospital affiliated with Shanghai Jiao Tong University [(2019) NLS No. (85)] and were performed in accordance with the tenets of the Declaration of Helsinki and its later amendments.

2.2 | Animals

Male db/db T2DM mice (BKS-Leprem2Cd479/Gpt, [Lepr] ko/ko, 12 weeks of age, plasma glucose concentration >33.3 mmol/L) and their age- and sex-matched, non-diabetic, healthy littermates were purchased from GemPharmatech. Co., Ltd (Nanjing, China). Experiments involving animals were performed according to the regulations of the Animal Care Committee of Shanghai Jiao Tong University, School of Medicine (SJTUSM). All experimental protocols were approved by the Institutional Animal Care and Use Committee of the SJTUSM.

2.3 | Induction of cutaneous wounds and treatment

All mice were shaved dorsally. The dorsal surface of the skin was sterilised with povidone-iodine and erased with alcohol cotton ball after anaesthetic induction with isoflurane. Subsequently, the mice were subjected to excisional wounding with a sterile 6 mm punch biopsy tool. Normal saline-treated wild-type control mice (WT-NS, n = 24) and diabetic control mice (db/db-NS, n = 24) were topically applied with 20 μL normal saline (NS) every 24 hours for 10 consecutive days. The diabetic experimental mice (db/db-PM, n = 24) were topically applied with PM (Sigma, P9158-1G) dissolved in normal saline (100 μM, 20 μL) at the same points in time. Finally, the wound was covered with a transparent dressing (3M, 1624W), which was replaced every day until day 10 post-injury.

2.4 | Analysis of the wound closure rate

On days 0, 1, 3, 5, 7, 10, and 14 post-injury, the mice were anaesthetised using isoflurane. To analyse the closure rate, the wounds were photographed at the specified time points. ImageJ software (National Institutes of Health) was performed to measure the wound areas.

2.5 | Preparation of wound tissue samples and histological evaluation

Human specimens were obtained as described above. Mice wound tissue samples were excised at 3, 7, 10, and 14 days after wounding. About 5 mm from the edge of the wound, the entire wound of mouse was removed. Samples were divided into two groups. Half of the samples were stored at −80°C. The other half of the samples were fixed using 10% formalin buffer for 24 hours. The fixed tissues were embedded in paraffin and sectioned to a thickness of 5 μm using a microtome. The sections were stained with haematoxylin and eosin (H&E) for histological evaluation.

2.6 | Immunohistochemistry

Human specimen sections were deparaffinised and rehydrated. Antigen retrieval was performed using 10 mM citrate sodium buffer (10 minutes at 100°C). Endogenous peroxidase was blocked by 3% hydrogen peroxide. At room temperature, the non-specific staining was blocked with 5% BSA for 1 hour. The sections were then incubated overnight with primary antibodies at 4°C. The primary antibodies are anti-MGO-AGEs (1:1000; Biosciences, Inc., SMC-516D, Canada) and anti-GLO1 (1:500; Santa Cruz, sc-133144). Subsequently, the sections were incubated with a horseradish peroxidase-conjugated secondary antibody (K5007, Dako, Denmark). 3,3′-diaminobenzidine was used for chromogenic development. Then, the sections were counterstained with haematoxylin. Three sections from each human were examined. Under the microscope, brown granules were positive. Images were taken in six fields per section (×100 and ×400 magnification).

2.7 | Cell culture, assessment of differentiation, and MGO stimulation

Human monocytic THP-1 cell line was purchased from the Cell Bank of the Chinese Academy of Sciences (Shanghai, China). The cells were cultured in a 37°C incubator under 5% CO_2 in RPMI 1640 medium (Thermo, 11875093) supplemented with 10% foetal bovine serum (Thermo, 10099141C). To induce differentiation of macrophages, the cells were cultured in the presence of phorbol 12-myristate 13-acetate (100 ng/mL, Sigma, P1585-1MG) for 24 hours. Lipopolysaccharide (100 ng/mL; SIGMA, L4391-1MG) was applied for 24 hours to induce the differentiation of macrophages into an M1-like phenotype. Interleukin 4 (20 ng/mL;

PeproTech, 200-04-20) and interleukin 13 (20 ng/mL; PeproTech, 200-13-20) were applied for 24 hours to induce the differentiation of macrophages into an M2-like phenotype. MGO (Sigma, M0252-25ML) at a concentration of 10 μM was used to reflect the estimated MGO levels in the plasma of T2DM patients. PM (Sigma, P9158-1G) at a concentration of 100 μM was used to quench MGO. MGO (10 μM) or MGO (10 μM) + PM (100 μM), using H_2O as a control, was applied to THP-1-derived macrophages in serum-free RPMI 1640 for 24 hours.

2.8 | Immunoblotting analysis

Immunoblotting analyses were performed as described previously.[27,28] In brief, total protein was extracted from the THP-1 macrophages and the mouse wound tissues. Equal amounts of denatured protein (20 μg) were separated by SDS-PAGE. Subsequently, the proteins were transferred to polyvinylidene fluoride membranes (Merck Millipore, ISEQ00010). The membranes were then incubated overnight with primary antibody at 4°C. The primary antibodies are MGO-derived AGEs (1:1000; StressMarq, SMC-516D), GLO1 (1:500; Santa Cruz, sc-133144), the macrophage-specific antigen marker F4/80 (1:1000; AbD Serotec, MCA497GA), and β-actin (1:10000; Proteintech, 66 009-1-Ig-100 μL). After washing with TBST, the membranes were incubated with horseradish peroxidase-conjugated specific secondary antibody, either anti-mouse immunoglobulin G (IgG) (1:3000, CST 7076S) or anti-rat IgG (1:3000, CST 7077S) for 1 hour at room temperature. The proteins were visualised via electrochemiluminescence (ECL) using a commercially available kit (Merck Millipore, WBKLS0100). Quantification was performed using a densitometer.

2.9 | Flow cytometry

The percentage of phagocytic cells was determined for each sample by evaluating the cellular endocytosis of 1 μm sized carboxylate-modified microspheres (Thermo Fisher Scientific, F8814). The microspheres were added to the cell cultures (~0.5×10^6 cells/mL) at a ratio of 30 microspheres per cell. The cultures were maintained at 37°C for 1 hour and washed three times with pre-cooled phosphate-buffered saline (PBS; Thermo Fisher Scientific, Inc., 10010023); the cells were harvested by trypsinization. The percentage of phagocytic cells was analysed by flow cytometry (BD LSRFortessa X-20 cell analyser).

2.10 | Immunofluorescence

The cells were seeded in glass slides (Merck Millipore, PEZGS0816), and immunostaining was performed using an anti-MGO-derived AGE antibody (1:200; StressMarq, SMC-516D). The samples were incubated with a fluorescent-conjugated secondary antibody (1:500; Invitrogen, Alexa Fluor 488 goat anti-mouse, A11001) at room temperature for 1 hour, followed by the addition of ProLong Gold Antifade Mountant with DAPI (Invitrogen, P36931) to label cell nuclei. The sections were visualised using an ultra-high resolution scanning confocal microscope (Leica TCS Sp8 STED, Germany).

2.11 | Enzyme-linked immunosorbent assay

Tumour necrosis factor alpha (TNF-α) (SXM063), interferon gamma (IFN-γ) (SXM021), interleukin 12 (IL-12) (SXM036), interleukin 10 (IL-10) (SXM035), and interleukin 6 (IL-6) (SXM032) levels in the wound tissues protein extracts of mice were quantified according to the manufacturer's instructions (Senxiong Biotech, Shanghai, China). The total protein concentration of mice wound tissues were measured in advance.

2.12 | Statistical analysis

All experiments were reduplicated not less than three times. Comparisons between two groups were conducted using Student's t tests. Comparisons among multiple groups were conducted via one-way analysis of variance. The GraphPad prism 7 software (GraphPad Software, La Jolla, California) was performed for statistical analysis. Statistical significance was established for P values <.05. All values are shown as the means ± SDs.

3 | RESULTS

3.1 | The accumulation of AGEs derived from MGO is increased in human diabetic skin and wound tissue

Considering that the level of MGO in serum cannot accurately reflect the level of MGO in the skin and wound tissue, quantifying AGEs derived from MGO may more accurately reflect the consequences of altered MGO concentrations. Thus, we investigated the expression of AGEs derived from MGO through immunohistochemical labelling. We found that the accumulation of

MGO-derived AGEs in the diabetic skin and wound tissue samples was increased. In contrast, fewer MGO-derived AGEs were observed in the non-diabetic skin and wound samples (Figure 1A,B).

3.2 | The expression of GLO1 is decreased in human diabetic skin and wound tissue

Because of the potentially harmful physiological effects of MGO, MGO detoxification is essential. Through immunohistochemical analysis, we found that GLO1 expression was more abundant in non-diabetic skin and wound tissue than in diabetic tissues, the latter of which exhibited significantly reduced GLO1 levels (Figure 2A,B). This decreased expression of GLO1 can at least partially explain the increase in AGEs derived from MGO in the diabetic skin and wound tissue.

3.3 | PM accelerates wound healing and improves delayed macrophage infiltration in diabetic mice

Diabetic wounds treated topically with PM exhibited significantly faster rates of closure (Figure 3A,B), and more granulation tissue was observed on day 7 after injury (Figure 3C). Wound macrophage infiltration was assessed by immunoblotting analysis to quantify the expression of F4/80. On day 7 post-wounding, the WT-NS group displayed a high level of F4/80 expression, whereas the db/db-NS group hardly expressed F4/80, and the expression of F4/80 in the db/db-PM group was partially restored (Figure 3D,E). On day 14 post-wounding, the WT-NS and db/db-PM groups rarely expressed F4/80,

whereas the db/db-NS group showed a high level of F4/80 expression (Figure 3F,G). These findings suggest that administration of PM can improve the infiltration and loss of macrophages during wound healing in diabetic mice.

3.4 | PM reduces the accumulation of MGO-derived AGEs in vivo and in vitro

To verify whether PM could reduce the accumulation of MGO-derived AGEs in diabetic wounds, we used immunoblotting experiments to evaluate the expression of AGEs derived from MGO. We collected the wound tissue of each group on day 7 post-wounding and extracted the total protein for immunoblotting analysis. The outcomes of the immunoblotting experiments suggested that compared with the WT-NS group, the glycation of proteins in the db/db-NS group was enhanced at different molecular weights; however, this was ameliorated in the db/db-PM group after topical application of PM, with concentrations equivalent to those of the WT-NS group (Figure 4A). In the In vitro experiments, compared with the control group, enhanced protein glycation of THP-1 M1-like macrophages was observed at different molecular levels in the MGO-treated group, whereas the level of protein glycation in the group that received MGO + PM was equivalent to that of the control group (Figure 4B). Consistent with the immunoblotting results, the immunofluorescent labelling experiments showed similar changes in the concentrations of MGO-derived AGEs in the control, MGO-treated, and MGO + PM-treated groups. These findings confirm that the changes in glycated proteins occurred not only in the cytoplasm, but also at the level of the cell membrane and nucleus (Figure 4C).
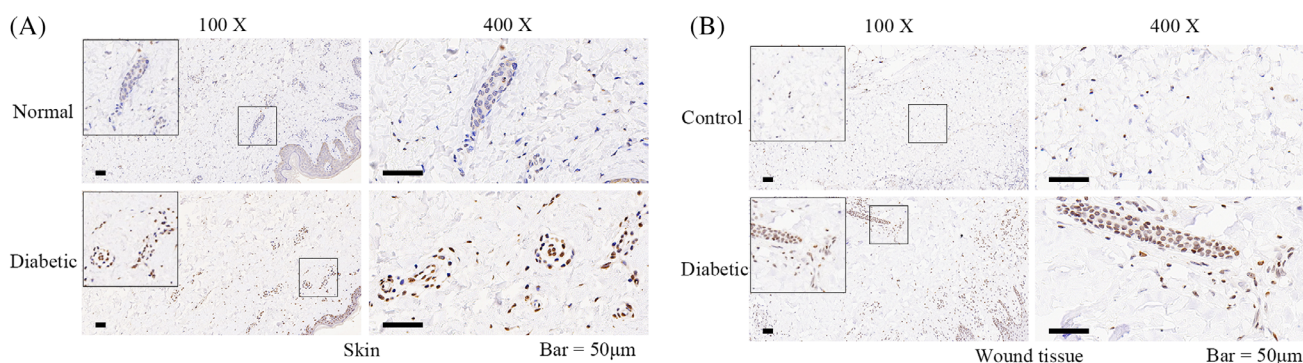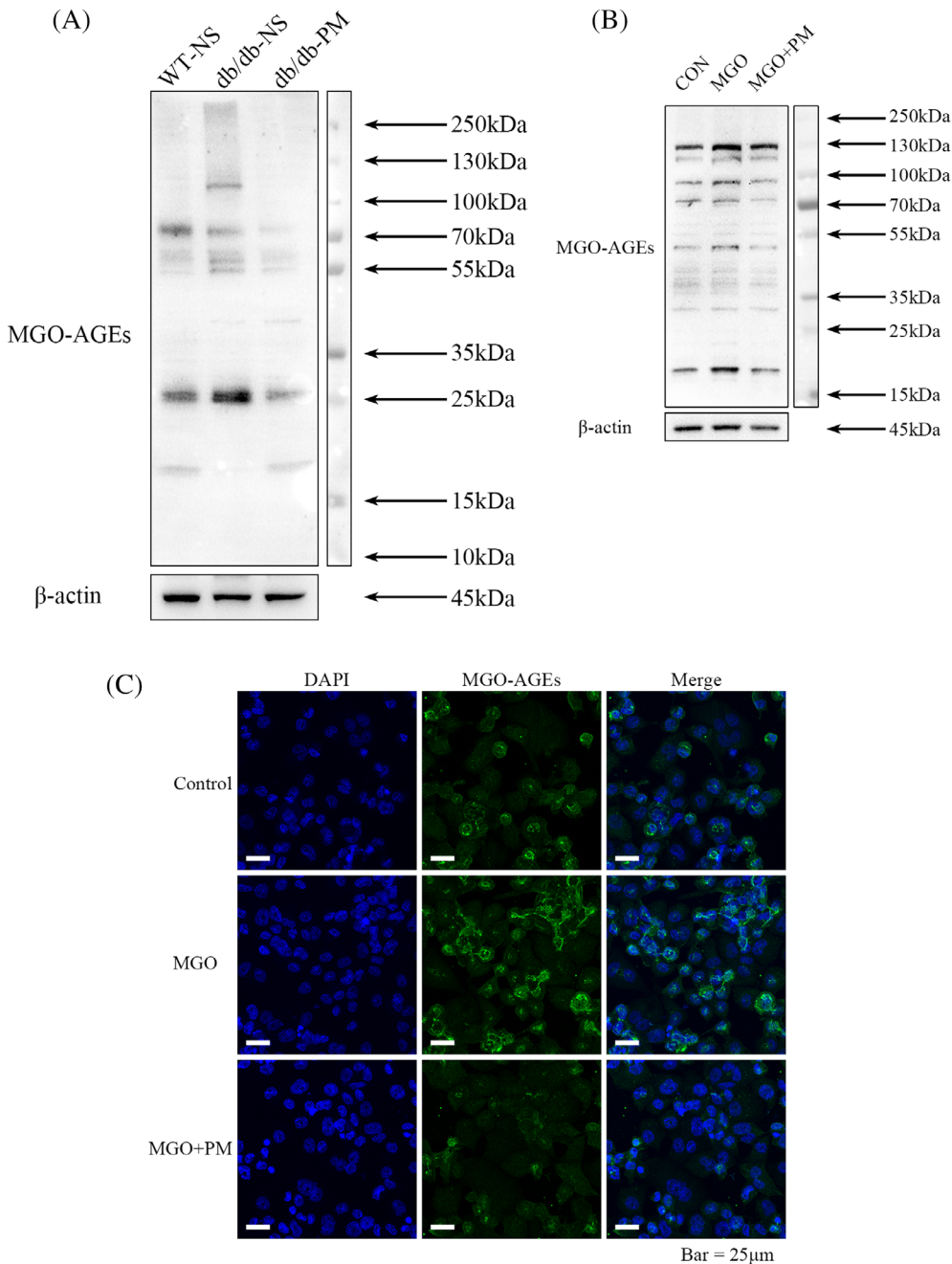

FIGURE 1 The accumulation of advanced glycation end products (AGEs) derived from methylglyoxal (MGO) in human diabetic skin and wound tissue. A, The expression of AGEs derived from MGO in normal and diabetic skin of human through immunohistochemical labelling. B, The expression of AGEs derived from MGO in non-diabetic (control) and diabetic (diabetic) wound tissues of human through immunohistochemical labelling. Representative images of three independent experiments (×100 and ×400). Scale bar = 50 μm
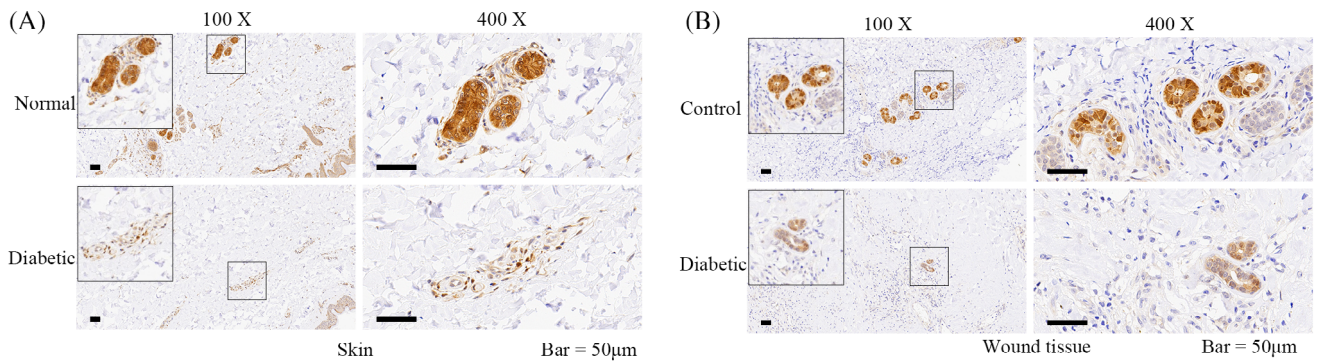
FIGURE 2 The expression of glyoxalase 1 (GLO1) in human diabetic skin and wound tissue. A, The expression of GLO1 in normal and diabetic skins of human through immunohistochemical labelling. B, The expression of GLO1 in non-diabetic (control) and diabetic (diabetic) wound tissues of human through immunohistochemical labelling. Representative images of three independent experiments (×100 and ×400). Scale bar = 50 μm
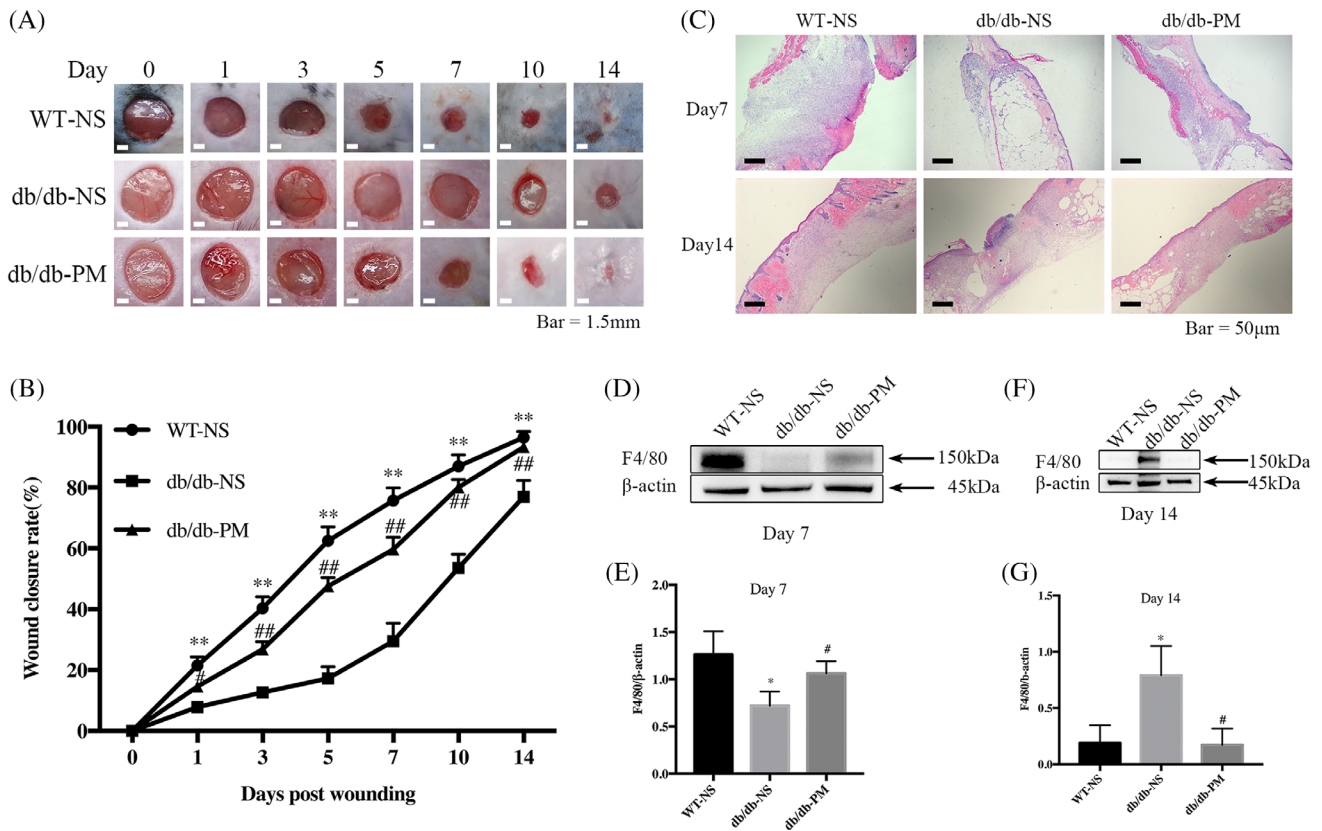
FIGURE 3 Topical application of pyridoxamine (PM) accelerates wound healing and improves delayed macrophage infiltration in diabetic mice. WT-NS (normal saline-treated wild-type control mice). db/db-NS (normal saline-treated diabetic control mice). db/db-PM (pyridoxamine-treated diabetic experimental mice). A, Representative wounds images. Scale bar = 1.5 mm. B, Comparisons of the wound closure rate. **$P < .01$, the WT-NS group compared with the db/db-NS group. #$P < .05$, ##$P < .01$, the db/db-NS group compared with the db/db-PM group. n = 6. C, Representative images of granulation tissue stained with haematoxylin and eosin (×50). Scale bar = 50 μm. D and E, Levels of F4/80 in mice wounds tissue of each group on day 7 post-wounding were assessed by immunoblotting analysis. *$P < .05$ compared with the WT-NS group. #$P < .05$ compared with the db/db-NS group. n = 3. F and G, Levels of F4/80 in wounds tissue of each group on day 14 post-wounding were assessed by immunoblotting analysis. *$P < .05$ compared with the WT-NS group. #$P < .05$ compared with the db/db-NS group. n = 3. Proteins levels were normalised to β-Actin levels

(A)

(B)

(C)

Bar = 25μm

3.5 | PM decreases the expression of GLO1 in vivo and in vitro

To evaluate whether the application of PM would augment GLO1 expression, thereby accelerating the detoxification of MGO, we used western blot analysis to evaluate the GLO1 concentrations. The wound tissue of each group was collected on day 7 post-wounding and the total protein was extracted. Surprisingly, the western blot analysis confirmed decreased GLO1 protein expression in diabetic wound tissue after treatment with PM (Figure 5A,B). Consistently, when THP-1 M1-like macrophages were cocultured with MGO and PM, the GLO1 levels were

down-regulated compared with the control and MGO groups (Figure 5C,D).

3.6 | PM improves the impairment of macrophage phagocytosis induced by MGO in vitro

To verify whether pathophysiological concentrations of MGO would affect the phagocytic function of macrophages, we first used flow cytometry to confirm that the administration of 10 μM MGO caused a decrease in the phagocytic function of THP-1 M1-like macrophages
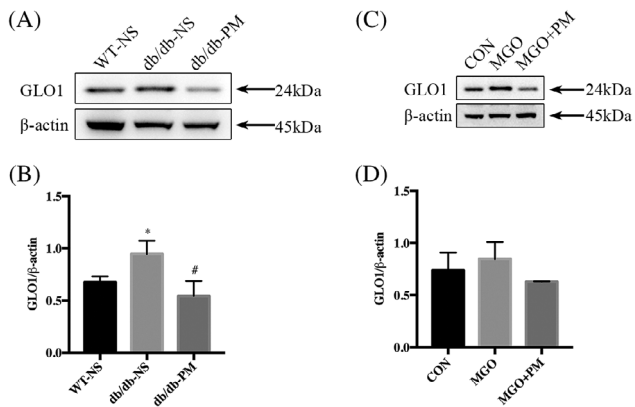
FIGURE 5 Pyridoxamine (PM) decreases the expression of glyoxalase 1 (GLO1) in diabetic wounds and M1 macrophages. WT-NS (normal saline-treated wild-type control mice). db/db-NS (normal saline-treated diabetic control mice). db/db-PM (pyridoxamine-treated diabetic experimental mice). Cells were treated with MGO (10 μM) or MGO (10 μM) + PM (100 μM), using H_2O as control, for 24 hours. A and B, Levels of GLO1 in mice wounds tissue protein of each group on day 7 post-wounding were assessed by immunoblotting analysis. *$P < .05$ compared with the WT-NS group. #$P < .05$ compared with the db/db-NS group. n = 3. C and D, Levels of GLO1 in M1 macrophages of each group were assessed by immunoblotting analysis. n = 3. Proteins levels were normalised to β-actin levels

induced by LPS (Figure 6C,D), without affecting the functions of THP-1 M0-like macrophages (Figure 6A,B) or THP-1 M2-like macrophages (Figure 6E,F) induced by PMA and IL-4 and IL-13, respectively. Secondly, we found that when PM (100 μM) and MGO (10 μM) were coincubated with M1-like macrophages, the altered percentages of phagocytic cells could be rescued and restored to a level comparable to that in the control group (Figure 6G,H).

3.7 | Topical application of PM alleviates excessive inflammation in vivo

To observe the outcome of inflammation during wound healing after the topical application of PM, we collected mouse wound tissues from day 3, day 7, and day 10 after wounding in each group, extracted the total protein content, and measured the protein concentrations via enzyme-linked immunosorbent assays. The concentrations of TNF-α (Figure 7A), IFN-γ (Figure 7B), IL-6 (Figure 7C), IL-12 (Figure 7D), and IL-10 (Figure 7E) were quantified separately, and we calculated the IL12/10 ratios (Figure 7F) at three time points after wounding. We observed that the expression of TNF-α and IL-6 in the WT-NS group was higher on day 3 post-injury, then gradually decreased, whereas the expression

levels in the db/db-NS group remained at a high level on day 10 post-injury. The expression of IFN- γ in the WT-NS group remained at a low level at various time points post-injury, whereas its expression in the db/db-NS group reached a high level on day 7 after injury. Similarly, after wounding, the db/db-NS group exhibited a higher IL-12/IL-10 ratio than the other two groups, and the ratio peaked on day 7.

4 | DISCUSSION

Glycation, a prevalent non-enzymatic covalent modification, results in the accumulation of proteins; it is the hallmark of diabetes and is associated with an array of other pathophysiologies,[29,30] including certain cancers and age-related changes.[31] Increased levels of the metabolite MGO have also been reported in patients with T2DM.[32] Our study showed that in diabetic wounds, the production of MGO is up-regulated, whereas the expression of GLO1 is decreased; thus, there was a disequilibrium between MGO and its metabolic enzyme GLO1. We observed that disrupting MGO accelerated the healing rate of diabetic wounds, which might be mediated through the reduction of MGO-related stress, and the improved migration of macrophages and the restoration of their phagocytic and secretory functions.

Previous studies have shown that MGO is an important pathological factor that contributes to the impairment of mechanisms that promote diabetic wound healing.[8,13] First, we confirmed that the concentration of AGEs derived from MGO in the skin and wound tissue of those with T2DM was increased, which reflects the abnormal accumulation of MGO and indicates that the healing microenvironment of the diabetic wound had been altered. It has been reported that impaired wound healing associated with ageing is relevant to lessened GLO1 expression.[33] We confirmed these results, as we found that in T2DM, the expression of GLO1 in the skin and wound tissue was reduced.

A previous report demonstrated that PM enhanced GLO1 activity in the erythrocytes of diabetic rats,[34] and in a diabetic mouse cutaneous wound model, the clearance of MGO through the induction of GLO1 was shown to promote wound healing.[14] However, we believe that the direct quenching of MGO through the administration of PM can alleviate MGO-associated cellular stress more quickly, and the use of PM seems more clinically valuable. Interestingly, our study found that the expression of GLO1 in wound tissue of diabetic mice and THP-1 M1-like macrophages decreased after the application of PM, although this might have been due to the direct quenching of MGO by PM, thereby reducing the need to
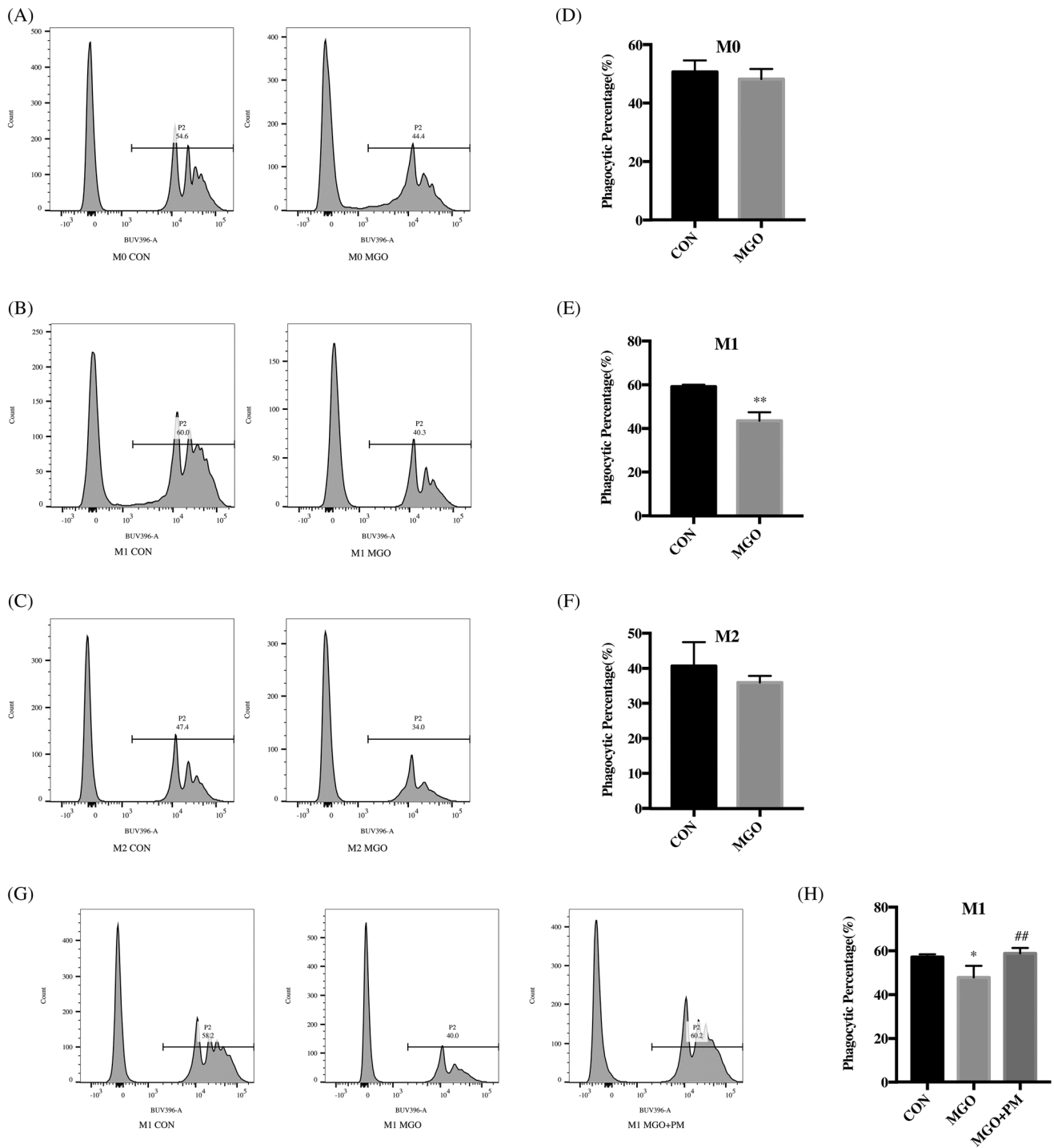
FIGURE 6 Pyridoxamine (PM) improves the impairment of M1 macrophages phagocytosis induced by methylglyoxal (MGO). Cells were treated with MGO (10 μM, using H_2O as control) for 24 hours. M1 macrophages were treated with MGO (10 μM) or MGO (10 μM) + PM (100 μM), using H_2O as control, for 24 hours. A-C, Representative results of phagocytosis percentage. D-F, Phagocytosis percentage was analysed by flow cytometry. **$P < .01$ compared with the control group. n = 3. G, Representative images of phagocytosis percentage. H, Phagocytosis percentage was analysed by flow cytometry. *$P < .05$ compared with the control group. ##$P < .01$ compared with the MGO group. n = 4

produce more GLO1 for MGO detoxification. Indeed, PM is currently considered the most important scavenger of MGO,[35] and the beneficial effects of PM have been

demonstrated clinically. For example, in a phase II clinical trial, PM not only ameliorated kidney function, but it also inhibited the formation of AGEs in T2DM patients
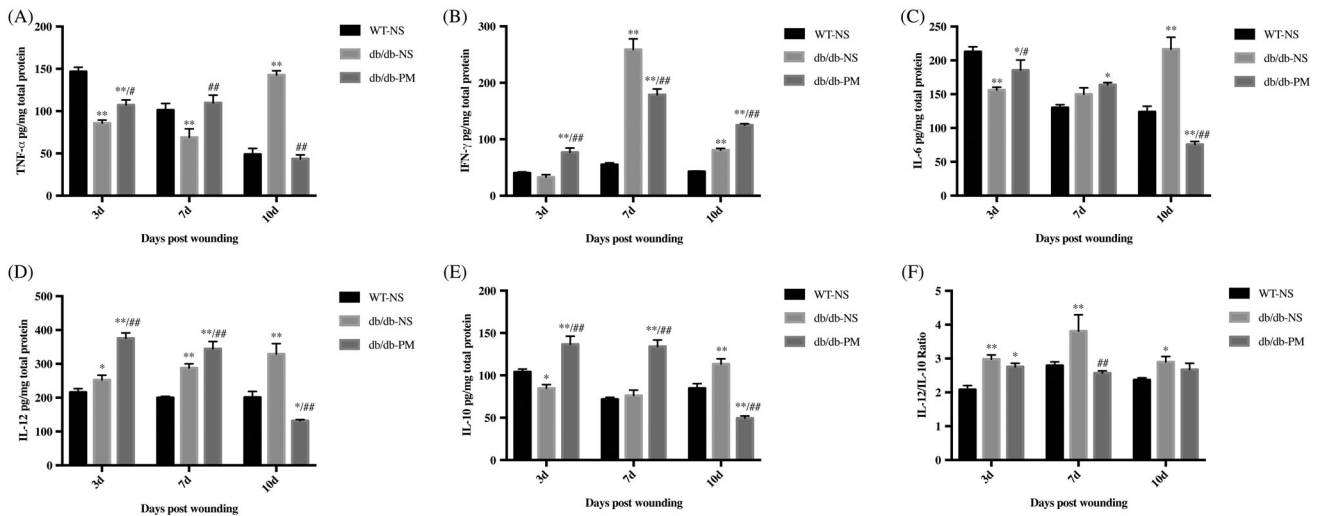
FIGURE 7 Topical application of pyridoxamine (PM) alleviates excessive inflammation in diabetic wounds. WT-NS (normal saline-treated wild-type control mice). db/db-NS (normal saline-treated diabetic control mice). db/db-PM (pyridoxamine-treated diabetic experimental mice). Mice wounds tissue was collected on days 3, 7, and 10 post-wounding of each group. A-E, The concentrations of TNF-α, IFN-γ, IL-6, IL-12, and IL-10 of each group were quantified by enzyme-linked immunosorbent assay. F, IL12/IL10. *P < .05, **P < .01 compared with the WT-NS group. #P < .05, ##P < .01 compared with the db/db-NS group. n = 3

with overt nephropathy.[24] In another clinical trial, the administration of PM reduced inflammation, pain, and the formation of AGEs in patients with osteoarthritis without any adverse effects.[25] Consistent with these previous observations, the topical application of PM to the wounds of type 2 db/db diabetic mice in this study reduced the accumulation of AGEs derived from MGO, and the rate of wound healing was restored to the rate seen in the WT mice.

The degree of macrophage infiltration affects the outcomes of wound healing[36] and the increased accumulation of AGEs in the wounds of diabetic mice has been shown to affect the timely infiltration of macrophages.[21] Our study indicated that the quantity of macrophages in the wounds of the diabetic mice was lower than that in the wounds of WT control mice during tissue regeneration phases, whereas the quantity remained at apparently greater levels in the tissue during the remodelling periods, which is consistent with former research studies.[27,37] After the topical application of PM, however, this dysfunction was improved. PM promotes macrophage infiltration in the process of diabetic wound healing, which is at least partly related to the reduced formation of MGO-derived AGEs. Phagocytosis of macrophages is considered to be crucial for the resolution of inflammation and the initiation of wound repair.[19,38] In vitro, we discovered that the phagocytic function of M1 macrophages was damaged by MGO, which could be reversed by the administration of PM. Interestingly, the phagocytosis of macrophages with an M0 or M2 phenotype was not affected by MGO. It has been reported that M1 macrophages mainly promote

inflammation, phagocytosis, and sterilisation, whereas M2 macrophages mainly involved in the resolution of inflammation and the promotion of mechanisms resulting in wound closure.[15] These functional differences may explain why the phagocytic functions of M0- and M2-type macrophages were not significantly disrupted by MGO. These experiments contribute to the mechanistic understanding of the role of topically applied PM in the regulation of macrophage dysfunction to accelerate the rate of wound healing in diabetic mice. Besides, the phenotype of macrophages in the wound is affected by its function and local environment.[15] Therefore, we paid more attention to the study of macrophage function here.

Voll et al demonstrated that the coculture of LPS-activated macrophages with apoptotic lymphocytes inhibited the release of pro-inflammatory cytokines such as TNF-α from macrophages and increased the expression of anti-inflammatory mediators.[39] In our animal experiments, the concentrations of inflammatory factors in the wound tissue of the db/db-PM group were higher than those in the db/db-NS group in the early stage of tissue repair. However, in the late stage of repair, the expression of inflammatory factors in the db/db-PM group decreased significantly, whereas the concentrations of inflammatory factors in the db/db-NS group remained at a high level. Thus, the topical application of PM promoted early-stage inflammation and alleviated late-stage inflammation in the wound healing process of diabetic mice, facilitating the transition from inflammation to tissue repair, possibly by ameliorating the dysfunction of macrophages.

5 | CONCLUSION

In conclusion, based on our experiments, there exists an imbalance between MGO and its metabolic enzyme GLO1. PM application directly quenches MGO, reducing MGO-mediated stress and macrophage dysfunction, promoting the formation of granulation tissue, and accelerating wound closure. Future studies should focus on the underlying mechanisms of these relationships in the healing of diabetic wounds. Once formed, AGEs are stable and the process is difficult to reverse; thus, targeting MGO, the precursor of AGEs, may be a feasible and viable method to reduce their accumulation. Ultimately, the MGO scavenging properties of PM provide new insights into a possible therapy to treat diabetic wounds, and further exploration could extend the pharmacological applications of PM for clinical treatment.

CONFLICT OF INTEREST
The authors have no conflicts of interest to declare.

DATA AVAILABILITY STATEMENT
The data that support the findings of this study are available from the corresponding author upon reasonable request.

ETHICS STATEMENT
All procedures involving human subjects were approved by the Ethics Review Board of Ruijin Hospital affiliated with Shanghai Jiao Tong University [(2019) NLS No. (85)] and were performed in accordance with the tenets of the Declaration of Helsinki and its later amendments. Each patient provided informed consent. Experiments involving animals were performed according to the regulations of the Animal Care Committee of Shanghai Jiao Tong University, School of Medicine (SJTUSM). All experimental protocols were approved by the Institutional Animal Care and Use Committee of the SJTUSM.

ORCID
Minfei Jiang https://orcid.org/0000-0002-4919-8551
Yiwen Niu https://orcid.org/0000-0002-5870-3089
Shuliang Lu https://orcid.org/0000-0001-9476-2564

REFERENCES
1. International Diabetes Federation. *IDF Diabetes Atlas.* 9th ed. Brussels, Belgium: IDF; 2019 https://www.diabetesatlas.org.
2. Amoah VMK, Anokye R, Acheampong E, Dadson HR, Osei M, Nadutey A. The experiences of people with diabetes-related lower limb amputation at the Komfo Anokye Teaching Hospital (KATH) in Ghana. *BMC Res Notes.* 2018;11(1):66.
3. Rabbani N, Xue M, Thornalley PJ. Methylglyoxal-induced dicarbonyl stress in aging and disease: first steps towards glyoxalase 1-based treatments. *Clin Sci (Lond).* 2016;130(19):1677-1696.
4. Schalkwijk CG, Stehouwer CDA. Methylglyoxal, a highly reactive dicarbonyl compound, in diabetes, its vascular complications, and other age-related diseases. *Physiol Rev.* 2020;100(1):407-461.
5. Thornalley PJ. Dicarbonyl intermediates in the Maillard reaction. *Ann N Y Acad Sci.* 2005;1043:111-117.
6. Ahmed N, Thornalley PJ, Dawczynski J, et al. Methylglyoxal-derived hydroimidazolone advanced glycation end-products of human lens proteins. *Invest Ophthalmol Vis Sci.* 2003;44(12):5287-5292.
7. Galligan JJ, Wepy JA, Streeter MD, et al. Methylglyoxal-derived posttranslational arginine modifications are abundant histone marks. *Proc Natl Acad Sci USA.* 2018;115(37):9228-9233.
8. Hanssen NMJ, Westerink J, Scheijen J, et al. Higher plasma methylglyoxal levels are associated with incident cardiovascular disease and mortality in individuals with type 2 diabetes. *Diabetes Care.* 2018;41(8):1689-1695.
9. Kinsky OR, Hargraves TL, Anumol T, et al. Metformin scavenges methylglyoxal to form a novel imidazolinone metabolite in humans. *Chem Res Toxicol.* 2016;29(2):227-234.
10. Rabbani N, Thornalley PJ. Dicarbonyl proteome and genome damage in metabolic and vascular disease. *Biochem Soc Trans.* 2014;42(2):425-432.
11. Sousa Silva M, Gomes RA, Ferreira AE, Ponces Freire A, Cordeiro C. The glyoxalase pathway: the first hundred years... and beyond. *Biochem J.* 2013;453(1):1-15.
12. Thornalley PJ. Glyoxalase I—structure, function and a critical role in the enzymatic defence against glycation. *Biochem Soc Trans.* 2003;31(Pt 6):1343-1348.
13. Berlanga J, Cibrian D, Guillen I, et al. Methylglyoxal administration induces diabetes-like microvascular changes and perturbs the healing process of cutaneous wounds. *Clin Sci (Lond).* 2005;109(1):83-95.
14. Li H, O'Meara M, Zhang X, et al. Ameliorating methylglyoxal-induced progenitor cell dysfunction for tissue repair in diabetes. *Diabetes.* 2019;68(6):1287-1302.
15. Hesketh M, Sahin KB, West ZE, Murray RZ. Macrophage phenotypes regulate scar formation and chronic wound healing. *Int J Mol Sci.* 2017;18(7):1545-1554.
16. Krzyszczyk P, Schloss R, Palmer A, Berthiaume F. The role of macrophages in acute and chronic wound healing and interventions to promote pro-wound healing phenotypes. *Front Physiol.* 2018;9:419.
17. Shapouri-Moghaddam A, Mohammadian S, Vazini H, et al. Macrophage plasticity, polarization, and function in health and disease. *J Cell Physiol.* 2018;233(9):6425-6440.
18. Atri C, Guerfali FZ, Laouini D. Role of human macrophage polarization in inflammation during infectious diseases. *Int J Mol Sci.* 2018;19(6):1801-1815.
19. Boniakowski AE, Kimball AS, Jacobs BN, Kunkel SL, Gallagher KA. Macrophage-mediated inflammation in normal and diabetic wound healing. *J Immunol.* 2017;199(1):17-24.

20. Wynn TA, Vannella KM. Macrophages in tissue repair, regeneration, and fibrosis. *Immunity*. 2016;44(3):450-462.

21. Wang Q, Zhu G, Cao X, Dong J, Song F, Niu Y. Blocking AGE-RAGE signaling improved functional disorders of macrophages in diabetic wound. *J Diabetes Res*. 2017;2017:1428537.

22. Voziyan PA, Hudson BG. Pyridoxamine as a multifunctional pharmaceutical: targeting pathogenic glycation and oxidative damage. *Cell Mol Life Sci*. 2005;62(15):1671-1681.

23. Vistoli G, Colzani M, Mazzolari A, et al. Quenching activity of carnosine derivatives towards reactive carbonyl species: focus on alpha-(methylglyoxal) and beta-(malondialdehyde) dicarbonyls. *Biochem Biophys Res Commun*. 2017;492(3):487-492.

24. Williams ME, Bolton WK, Khalifah RG, Degenhardt TP, Schotzinger RJ, McGill JB. Effects of pyridoxamine in combined phase 2 studies of patients with type 1 and type 2 diabetes and overt nephropathy. *Am J Nephrol*. 2007;27(6):605-614.

25. Garg S, Syngle A, Vohra K. Efficacy and tolerability of advanced glycation end-products inhibitor in osteoarthritis: a randomized, double-blind, placebo-controlled study. *Clin J Pain*. 2013;29(8):717-724.

26. Maessen DE, Brouwers O, Gaens KH, et al. Delayed intervention with pyridoxamine improves metabolic function and prevents adipose tissue inflammation and insulin resistance in high-fat diet-induced obese mice. *Diabetes*. 2016;65(4):956-966.

27. Yan J, Tie G, Wang S, et al. Diabetes impairs wound healing by Dnmt1-dependent dysregulation of hematopoietic stem cells differentiation towards macrophages. *Nat Commun*. 2018;9(1):33.

28. Liu D, Yang P, Gao M, et al. NLRP3 activation induced by neutrophil extracellular traps sustains inflammatory response in the diabetic wound. *Clin Sci (Lond)*. 2019;133(4):565-582.

29. Zheng Q, Omans ND, Leicher R, et al. Reversible histone glycation is associated with disease-related changes in chromatin architecture. *Nat Commun*. 2019;10(1):1289.

30. Harmel R, Fiedler D. Features and regulation of non-enzymatic post-translational modifications. *Nat Chem Biol*. 2018;14(3): 244-252.

31. Thornalley PJ, Langborg A, Minhas HS. Formation of glyoxal, methylglyoxal and 3-deoxyglucosone in the glycation of proteins by glucose. *Biochem J*. 1999;344(Pt 1):109-116.

32. Moraru A, Wiederstein J, Pfaff D, et al. Elevated levels of the reactive metabolite methylglyoxal recapitulate progression of type 2 diabetes. *Cell Metab*. 2018;27(4):926-934.e928.

33. Fleming TH, Theilen TM, Masania J, et al. Aging-dependent reduction in glyoxalase 1 delays wound healing. *Gerontology*. 2013;59(5):427-437.

34. Nagaraj RH, Sarkar P, Mally A, Biemel KM, Lederer MO, Padayatti PS. Effect of pyridoxamine on chemical modification of proteins by carbonyls in diabetic rats: characterization of a major product from the reaction of pyridoxamine and methylglyoxal. *Arch Biochem Biophys*. 2002;402(1):110-119.

35. Maessen DE, Stehouwer CD, Schalkwijk CG. The role of methylglyoxal and the glyoxalase system in diabetes and other age-related diseases. *Clin Sci (Lond)*. 2015;128(12):839-861.

36. Lucas T, Waisman A, Ranjan R, et al. Differential roles of macrophages in diverse phases of skin repair. *J Immunol*. 2010;184 (7):3964-3977.

37. Miao M, Niu Y, Xie T, Yuan B, Qing C, Lu S. Diabetes-impaired wound healing and altered macrophage activation: a possible pathophysiologic correlation. *Wound Repair Regen*. 2012;20(2):203-213.

38. Yang P, Wang X, Wang D, et al. Topical insulin application accelerates diabetic wound healing by promoting anti-inflammatory macrophage polarization. *J Cell Sci*. 2020;133 (19). https://doi.org/10.1242/jcs.235838.

39. Voll RE, Herrmann M, Roth EA, Stach C, Kalden JR, Girkontaite I. Immunosuppressive effects of apoptotic cells. *Nature*. 1997;390(6658):350-351.